TORSIONAL RESPONSE OF BUILDINGS TO STRONG EARTHQUAKE MOTIONS

by

Akenori Shibata*, Junichi Onose** and Toshio Shiga***

Synopsis. Presented are the results of non-linear response analysis of single-story unsymmetrical building models with bi-linear restoring force characteristics against idealized earthquake inputs. It is shown that the unsymmetry in strength as well as in stiffness has great influence on the non-linear torsional behavior. Also shown are the results of static and dynamic experiments of single-story unsymmetrical reinforced concrete bents. The properties of moment-rotation relation and the characteristics of torsional modes of vibration in the inelastic range are investigated in the experiments.

INTRODUCTION

Buildings unsymmetrical in plan and elevation or irregular in the arrangement of walls will undergo torsional vibration during earthquakes and damages on buildings will be considerably increased due to the effect of torsion. In fact, a number of torsional damages have been reported in the past earthquakes.

The majority of previous investigations on this subject has dealt with the linear torsional vibration. However, in consideration of the inelastic behavior of buildings subjected to severe earthquakes, it is of quite importance to investigate the non-linear torsional behavior of unsymmetrical buildings.

The former part of this paper describes on the non-linear torsional response of single-story unsymmetrical building models with bi-linear hysteretic restoring forces by the use of analog computer. The latter part describes on the results of the static and dynamic experiments of reinforced concrete unsymmetrical bents and discusses on several problems in constructing torsional vibration models for non-linear response analysis.

NON-LINEAR RESPONSE OF SINGLE-STORY UNSYMMETRICAL BUILDING

Building Models. Let a single-story building which is unsymmetrical in stiffness and strength be considered as shown in Fig. 1. The roof of the building is a square, rigid slab of $2l$ in width with uniformly distributed mass, m. The center of mass is situated at the geometrical center of the slab.

The equivalent torsional vibration model of the unsymmetrical building is shown in Fig. 2. The restoring force characteristics of columns in the x and y directions are represented by the four non-linear springs with elastic spring constants ${}_1k_x$, ${}_2k_x$, ${}_1k_y$, ${}_2k_y$ and yield shear forces ${}_1Q_{Yx}$, ${}_2Q_{Yx}$, ${}_1Q_{Yy}$, ${}_2Q_{Yy}$, respectively.

*Assistant Professor, Faculty of Engineering, Tohoku University
**Assistant, Faculty of Engineering, Tohoku University
***Professor, Faculty of Engineering, Tohoku University

The characteristics of non-linear springs are assumed to be of elasto-plastic type or of negative bi-linear type as shown in Fig. 3.

The torsional vibration model has three degrees of freedom and its motion is expressed completely by the displacement of the center of gravity (x,y) and the rotation about the center of gravity θ.

The degrees of unsymmetry in stiffness and strength in each direction are expressed by the following parameters.

$$\beta = {}_2k / {}_1k \qquad \text{: stiffness distribution} \qquad (1)$$

$$\gamma = {}_2Q_Y / {}_1Q_Y \qquad \text{: strength distribution} \qquad (2)$$

β or γ has a pair of values corresponding to the x and y directions and is written as $\beta\ (\beta_x, \beta_y)$ or $\gamma\ (\gamma_x, \gamma_y)$.

The total stiffness in the y direction $({}_1k_y + {}_2k_y)$ is always equal to $4\pi^2 m$ which is identical with the stiffness of the symmetrical model having the natural period of 1.0 sec. The ratio of total stiffness in the x direction to that in the y direction is denoted by the parameter α.

$$\alpha = ({}_1k_x + {}_2k_x) / ({}_1k_y + {}_2k_y) \qquad (3)$$

The total strength in a direction is expressed by the parameter C_Y.

$$C_Y = ({}_1Q_Y + {}_2Q_Y) / mg \qquad \text{: total yield level} \qquad (4)$$

The types of models considered in the analysis are as follows.

Model I : The unsymmetry in stiffness exists only in the y direction while there is no unsymmetry in the x direction.

Model II: The same amounts of unsymmetry in stiffness exist both in the x and y directions.

In Model I and Model II, the total stiffness and the total yield levels are the same for the x and the y directions. ($\alpha = 1.0$, $C_{Yx} = C_{Yy}$)

Model Ia: The unsymmetry in stiffness exist only in the y direction as in Model I. The difference from Model I is that the springs in the x direction remain always linear and yielding occurs only in the y direction and that the total stiffness in the x direction is varied as $\alpha = 1.0$, 0.5 and 0.

In Model Ia, vibrations in the x and y directions are independent each other and the input from the x direction has no influence on the response in the y direction.

Combination of stiffness distribution and strength distribution is considered to be an important factor affecting the non-linear torsional response. The following two cases are assumed in the analysis. Most cases encountered in ordinary buildings are considered to be situated between these two cases.

Case A : Yield shear of each spring is proportional to its elastic spring constant as shown in Fig. 3. ($\gamma = \beta$)

Case B : Yield shear of each spring is constant irrespective of its spring constant as shown in Fig. 3. ($\gamma = 1$)

Equations of Motion. Equations of motion of the torsional vibration model are expressed as follows. It is assumed that the ground motion has two components in the x and y directions and involves no rotational components.

$$
\begin{aligned}
m(\ddot{x}+\ddot{x}_0) &= -{}_1C_x \cdot {}_1\dot{\delta}_x - {}_2C_x \cdot {}_2\dot{\delta}_x - {}_1Q_x({}_1\delta_x) - {}_2Q_x({}_2\delta_x) \\
m(\ddot{y}+\ddot{y}_0) &= -{}_1C_y \cdot {}_1\dot{\delta}_y - {}_2C_y \cdot {}_2\dot{\delta}_y - {}_1Q_y({}_1\delta_y) - {}_2Q_y({}_2\delta_y) \qquad (5) \\
J\ddot{\theta} &= -{}_1C_x \cdot {}_1\dot{\delta}_x \cdot l + {}_2C_x \cdot {}_2\dot{\delta}_x \cdot l - {}_1C_y \cdot {}_1\dot{\delta}_y \cdot l + {}_2C_y \cdot {}_2\dot{\delta}_y \cdot l \\
&\quad - {}_1Q_x({}_1\delta_x) \cdot l + {}_2Q_x({}_2\delta_x) \cdot l - {}_1Q_y({}_1\delta_y) \cdot l + {}_2Q_y({}_2\delta_y) \cdot l
\end{aligned}
$$

where $\ddot{x}_o$ and $\ddot{y}_o$ denote the ground accelerations and ${}_i\delta$ denotes the displacement of each spring as follows.

$$
\begin{aligned}
{}_1\delta_x &= x + l\cdot\theta & {}_1\delta_y &= y + l\cdot\theta \\
{}_2\delta_x &= x - l\cdot\theta & {}_2\delta_y &= y - l\cdot\theta
\end{aligned} \qquad (6)
$$

${}_iQ({}_i\delta)$ denotes the restoring force function of each spring which depends on the displacement of spring ${}_i\delta$ as shown in Fig. 3. J denotes the moment of inertia of slab and equal to $2/3\ ml^2$. The damping terms are determined from ${}_ic = 1/20\pi \cdot {}_ik$, which gives 5% of critical damping for the symmetrical model.

Earthquake Inputs. To investigate the effect of torsion on the non-linear response, it is considered suitable to use the idealized ground motions having rather simple spectrum shapes. In this analysis, one to three half-sine acceleration pulses with the period of 1.0 sec and the maximum acceleration of 1.0g are used as earthquake inputs. It is assumed that in every case the x and y components of the earthquake input are the same and are acted upon the model simultaneously from the both direction so as to produce most severe torsional effect.

Response of Elasto-Plastic Unsymmetrical Model. The maximum displacements of springs and the maximum rotations for each case have been obtained by varying the total yield level by the use of analog computer.(1)

In Fig. 4 are shown the relations between the total yield level C_Y and the maximum displacements of flexible and stiff springs, ${}_1\delta_{max}$ and ${}_2\delta_{max}$, in the y direction for Model I in case of $\beta = 2$ subjected to one to three half-sine pulses. In Model I, the symmetrical springs in the x direction produce different plastic displacements due to the effect of the unsymmetry in the y direction. The values of maximum displacements in the x direction are very close to those in the y direction for $\beta = 2$.

In Figs. 5,6 and 7 are shown the C_Y-δ_{max} relations in the y direction for Model II and Model Ia ($\alpha = 1$ & 0) in case of $\beta = 2$ subjected to one half-sine pulse.

The maximum displacements of symmetrical models having the same yield levels are also shown in the figures by the dotted lines. The straight line ${}_i\delta_Y$ indicates the yield displacement corresponding to C_Y and the ratio of the maximum displacement to the yield displacement for the same yield level gives the ductility factor ${}_i\mu$ of each spring. Natural periods for torsional modes are 1.04sec and 0.57sec for Model I and Model Ia($\alpha = 1$), 1.09sec and 0.56sec for Model II and 1.14sec and 0.76sec for Model Ia($\alpha = 0$).

It is seen from Figs. 4 to 7 that the trends of C_Y-δ_{max} curves of

unsymmetrical models are similar to those of symmetrical models and the average values of ${}_1\delta_{max}$ and ${}_2\delta_{max}$ generally agree well with the maximum displacements of symmetrical models for the same yield levels.

It is found that the difference between ${}_1\delta_{max}$ and ${}_2\delta_{max}$ in the non-linear range are larger in Case A than in Case B, or in other words, the rotational motions in the non-linear range are greater in Case A than in Case B.

The amounts of rotation in the non-linear range are also affected in a complicated way by the input patterns and the total yield levels. By examining the most simple case of one half-sine pulse, however, several interesting trends on the relation between the maximum rotation θ_{max} and C_y can be seen as follows. In Model I and Model II, θ_{max} increases greatly with the decrease of C_y in Case A, while θ_{max} increases very little with the decrease of C_y in Case B. In Model Ia, the trends of θ_{max} are different according to the value of α. In the case of $\alpha = 1$ and 0.5, θ_{max} decreases rapidly and translational motions become dominant with the decrease of C_y both in Case A and Case B, while in the case of $\alpha = 0$ the trends of θ_{max} are the same as those in Model I and Model II.

It can be said from the above that the strength distribution and the properties of torsional resistance have great influence on the torsional behavior in the non-linear range.

The ductility factors ${}_i\mu$ vary significantly according to the strength distribution. Fig. 8 shows the variation of ductility factors of torsional model having a constant yield level with the strength distribution in case of Model II and Model Ia. It is seen that if an adequate strength distribution is selected, ductility factors of every spring can be made equal. For Model II and Model Ia, the value of γ for uniform μ are uniquely determined and are seen close to the ratios between the maximum shears in elastic response or the shear ratio for static force applied at the gravity center, for the range of yield levels producing moderate plastic deformation.

Further, it is recognized from the comparison of Model I and Model Ia ($\alpha = 1$) that the yielding in the one direction have effects on the response in the other direction and that it is unrealistic to treat the non-linear torsional vibrations in the x and y directions separately.

Response of Negative Bi-linear Unsymmetrical Model. When buildings are subjected to large plastic deformation under severe earthquakes, the restoring force-displacement relation will show negative bi-linear characteristics due to the effects of gravity loads, shear failure, buckling etc.
In the analized model, plastic spring constant ${}_ik_p$ is assumed to be -0.1 times the elastic spring constant for convenience of treatment as shown in Fig. 3. The collapse displacement of each spring for which the restoring force vanishes is designated by ${}_i\delta_c$.

Fig. 9 shows the C_y-δ_{max} relations for Model II. The critical yield levels for which either of springs attains the collapse displacement can be obtained from the intersecting points of C_y-δ_{max} curves and straight lines of δ_c. Table 1 shows the critical yield levels for Model I and Model II in case of $\beta = 2$. It is found that the critical yield levels for torsional models are generally higher than those for the symmetrical models in Case A, while close to those for the symmetrical models in Case B.

EXPERIMENTS OF SINGLE-STORY REINFORCED CONCRETE UNSYMMETRICAL BENTS

Test Specimens. Two types of specimens, A type and AE type, are considered. Both are single-story reinforced concrete bents composed of two framse in each direction x and y, and are similar to the analytical models as studied in the former part of this paper. The details of the test specimen are illustrated in Fig. 10.

In A type, the distribution of mass, stiffness and yield strength are uniform. So, there is no eccentricity. In AE type, the mass is uniformly distributed but the distribution of stiffness and yield strength are non-uniform. The eccentricity lies on the principal axis of y as shown in Fig. 10. The properties of the test specimen are shown in Table 2.

Torsional Stiffness of Buildings. In the analysis of torsional response, it is assumed that the torsional stiffness of building is generally determined from only the horizontal stiffness of columns and the torsional stiffness of columns is neglected, and that the above horizontal stiffness of columns is the value subjected to uni-axial bending. Therefore, the torsional stiffness of building is expressed by the following equation.

$$\mathcal{M} = \Sigma (k_x \cdot y^2 + k_y \cdot x^2) \qquad (7)$$

where $\mathcal{M}$: torsional stiffness of building
k_x, k_y : horizontal stiffness of column
x, y : distance from the center of rotation to the column

Actually, columns have torsional stiffness in themselves and are subjected to bi-axial bending and torsion when buildings undergo torsional vibration. Accordingly, the validity of the above assumption is one of the problems. To examine these, the static tests were carried out.

Experiments were divided into four steps with increasing maximum deflections. Each step is performed in the following order; first, translational displacement to the x direction, second, translational displacement to the y direction, and third, pure torsion about the center of gravity. The specimens were subjected to two cycle alternate loading under the appointed maximum deflection to obtain steady state hysteresis loop of each frame. The maximum displacements of frames attained in each step are made equal for both translational and pure torsional loadings.

The relations between torsional moment and rotation angle are presented in Fig. 12. The solid line shows the curve obtained from the experiment, $(M_t-\theta)$. The broken line shows the curve calculated from the equation (7) using the load-deflection curves in the x and y direction obtained from the static test, $(\bar{M}_t-\theta)$. The fine solid line shows the calculated curve using the equation (7) added by the calculated torsional resistance of column, $(\bar{M}_t+\bar{M}_c-\theta)$. The torsional resistance characteristics of columns are computed by the following method; the torsional stiffness in the elastic range is computed from the theory of St. Venant, and the yield torsional moment from the equation proposed by A.H. Mattock. These are shown in Fig. 11.

The results are summarized as follows.

1) In the range of small rotation angle, there is difference between $(M_t-\theta)$ and $(\bar{M}_t-\theta)$ in both A and AE type specimens. But the curves considering the torsional stiffness of columns $(\bar{M}_t+\bar{M}_c-\theta)$ agree well with the experimental

curves (M_t-θ). Consequently, when the rotation angle is in the small range, the torsional stiffness of building is expressed by the sum of the torsional stiffness of columns and the value from the equation (7).

2) In the range of large rotation angle, in A type specimen, ($\bar{M}_t$-θ) curve agrees well with the experimental curve (M_t-θ) in a whole. In AE type, however, there is considerable difference between the maximum torsional moment of ($\bar{M}_t$-θ) and that of (M_t-θ).

It is seen from the above results that the torsional stiffness of columns in the large amplitude is reduced in both A and AE type specimens and the torsional stiffness of building is expressed by the equation (7) in A type. But in case of AE type, the equation (7) is not valid. The value of the maximum torsional moment obtained from the experiment is smaller than that of calculated. It is inferred that this descrepancy is related to the fact that columns having larger cross section with multi-stage reinforcement show different behavior in uni-axial bending and bi-axial bending.

Modes of Torsional Vibration. The dynamic tests were carried out for the AE type specimen and the mode shapes under the steady state vibration were examined. The dynamic loading was performed with large scale shaking table. The specimen was shaked under the steady state vibration to a sinusoidal motion and was collapsed finally. The motion of the roof was measured with the specially designed rahmen type deflection transducers shown in Photo 1.

The results are presented in Fig. 13, Fig. 14 and Table 3. Fig. 13 shows the mode shapes in vibration and Fig. 14 illustrates the relation between the maximum displacement of the center of gravity, $\delta_{s\,max}$, and the distance of rotation center from the gravity center, ρ. The loading period and the others are shown in Table 3.

The value of ρ is a parameter corresponding to the degree of torsion and defined as the ratio of the displacement of gravity δ_s to the rotation angle θ. So, the smaller the value of ρ becomes, the larger the torsion. In the steady state vibration in the elastic range, ρ is determined from the torsional stiffness, the eccentricity and the ratio of the natural period of building to the loading period, T_{force}.

In Fig. 14, the computed value of ρ is also plotted. The computation is conducted as follows; the ratio of torsional stiffness to the horizontal stiffness and the eccentricity are those from elastic calculation, and to estimate the ratio of natural period of specimen to loading period, the equivalent stiffness from the static test is used.

The results are pointed out as follows.

1) In the test of the beginning to test 3-3, both the displacement of gravity center and the rotation angle are small. In test 3-4, it happened resonance and the specimen vibrated in large amplitude. It was presumed that the specimen yielded at resonance. The values of ρ obtained from experiments are in good agreement with the calculated values for the wide range of displacement including the state of resonance.

2) After the specimen yielded, it seemed that the torsional characteristics changed. In test 3-5 to 5-3, the displacements of gravity center and the rotation angles were both increased.

3) In test 6, the rotation angle was increased rapidly while the displacement of the gravity center were decreased inversely, and then the specimen was collapsed. It seemed that the change in the distribution of stiffness and strength were advanced for the unfavourable direction, so the eccentricity increased and the torsional stiffness decreased, and then collapse took place.

RESULTS AND CONCLUSIONS

The following remarks can be pointed out from the results of the analyses and experiments.

1) In the analysis of the non-linear torsional response, the ground motions from both the x and y directions should be considered simultaneously, since yielding in the one direction has effects on the response of the other direction.

2) It is seen from the response of elasto-plastic models that the distribution of strength as well as of stiffness has significant influence on the non-linear response. It is found that in the case in which the strength is proportional to the stiffness, rotational motions in the non-linear range are much greater than in the case in which the strength is constant irrespective of the stiffness.

3) Ductility factors in torsional buildings are differnt according to the strength distribution, and it is found that by selecting adequate relations between stiffness and strength, the distribution of ductility factor approaches to the uniform distribution.

4) The effect of torsion on the collapse phenomenon in negative bi-linear models was studied and it is shown that the critical yield strength for collapse is influenced by the strength distribution and that collapse will be easy to occur when rotational motions are dominant in the low yield strength.

5) It is found from the results of static test that the torsional stiffness of columns contributes to the torsional stiffness of building as a whole in the range of small rotation angle, while has little effect in the range of large rotation angle. It is also seen that the strength of columns will be different under uni-axial bending and bi-axial bending.

6) In the dynamic test, the change in the distribution of stiffness as well as of strength were observed. The ratio of rotational motion to translational motion increased with the increase of amplitude and the collapse occured in the torsional mode.

Reference.

1. T.Shiga, A.Shibata and J.Onose "Torsional Response of Buildings to Strong Motion Earthquakes" Proceedings of Japan Earthquake Engineering Symposium, October 1966
2. G.W.Housner and H.Outinen "The Effect of Torsional Oscillations on Earthquake Stresses" Bulletin of Seismological Society of America. July 1958
3. G.W.Housner "The Plastic Failure of Frames During Earthquakes" Proceedings of the Second World Conference on Earthquake Engineering 1960

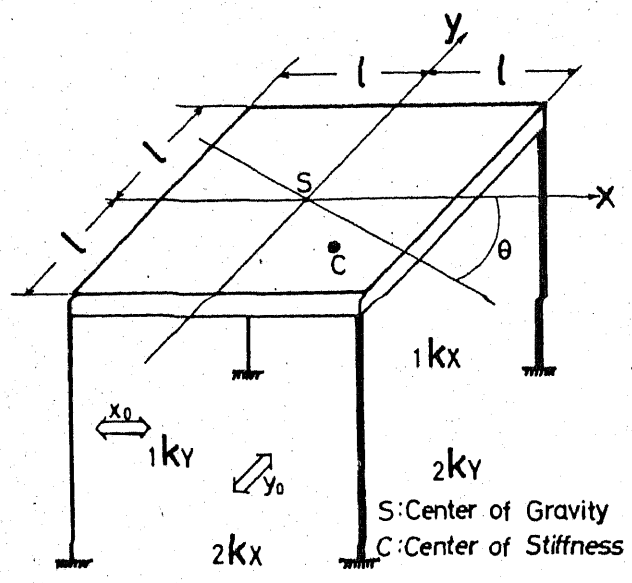

Fig.1 Single-Story Unsymmetrical Building

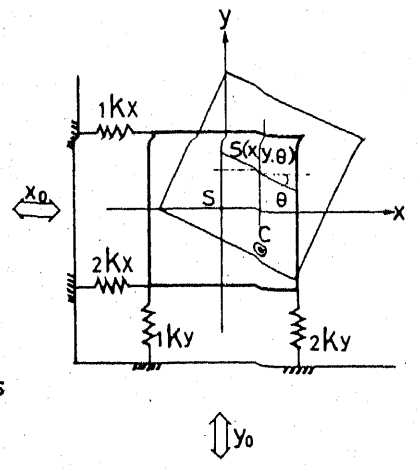

Fig.2 Torsional Vibration Model

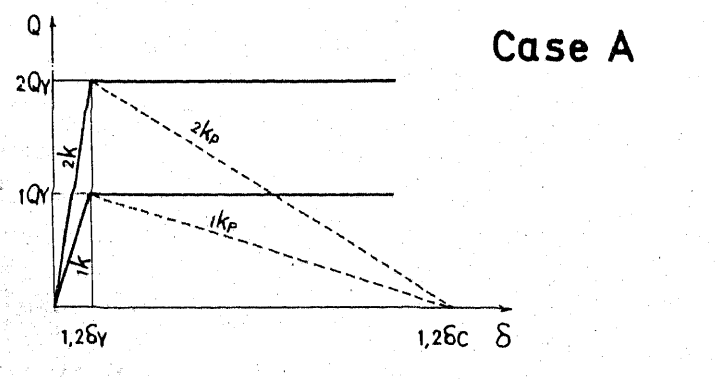

Case A

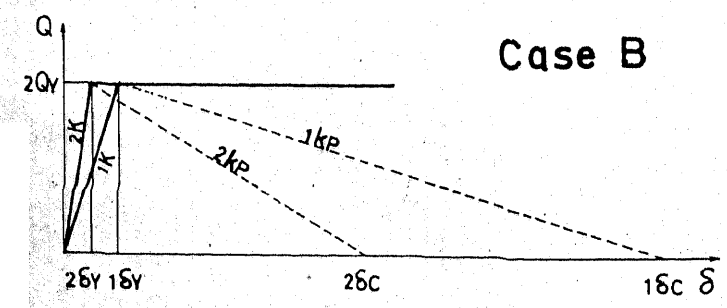

Case B

Fig.3 Resoring Force-Displacement Relations

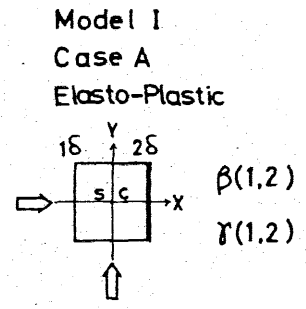

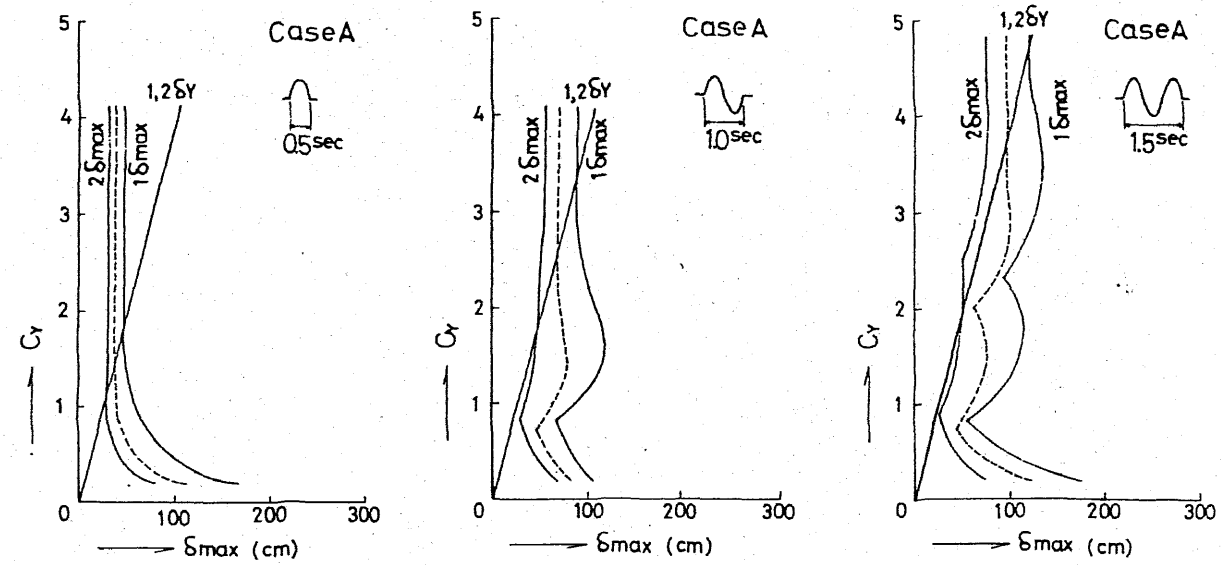

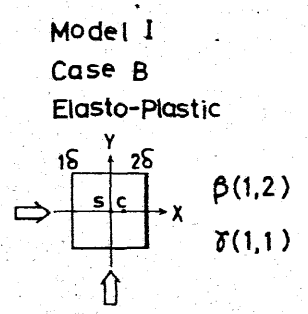

(------ : Symmetrical Model)

Fig. 4 Relation between Total Yield Lebel Cy and Maximum Displacement δmax in the y Direction (Model I)

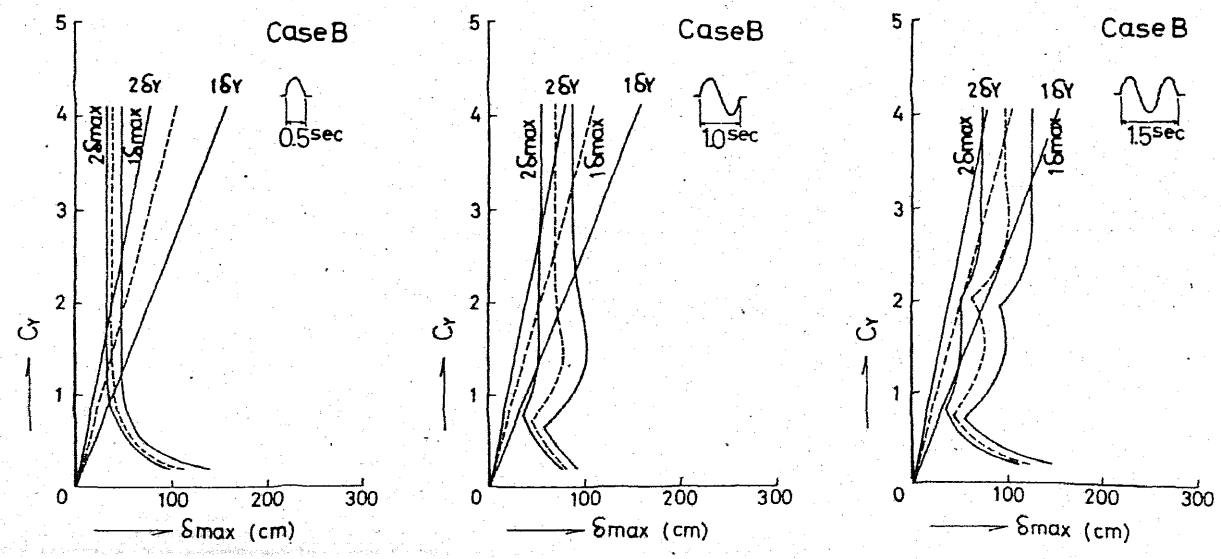

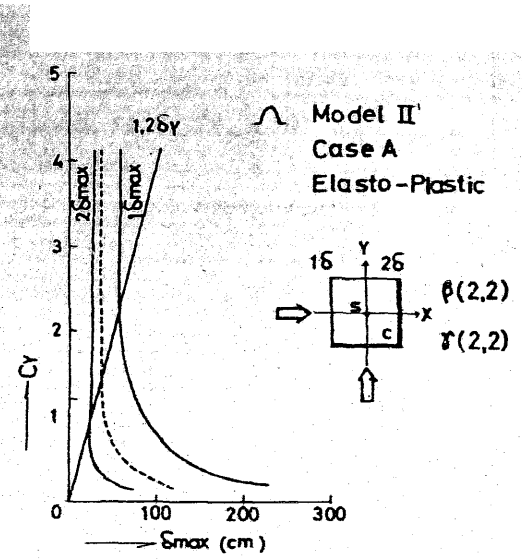

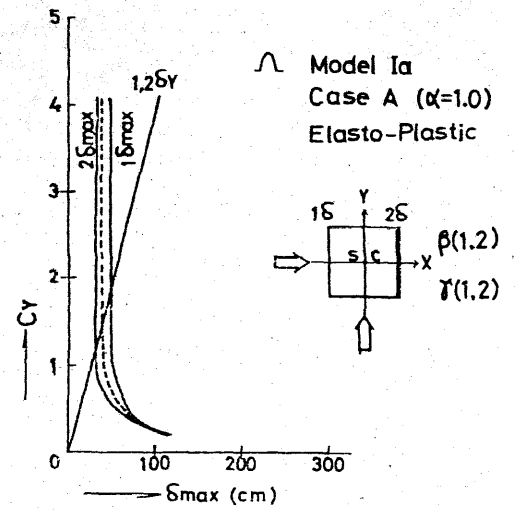

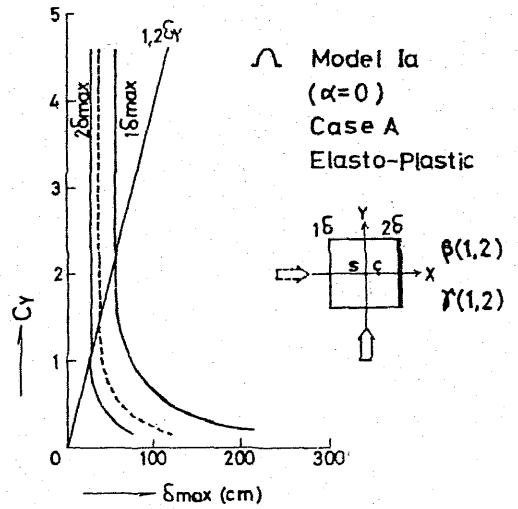

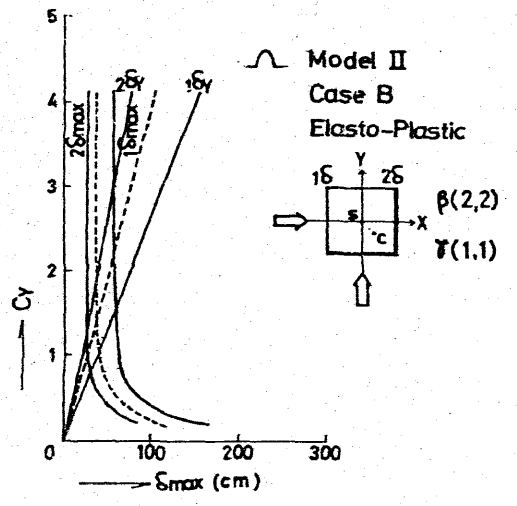

Fig.5 Relation between C_γ and δ_{max} (Model II)

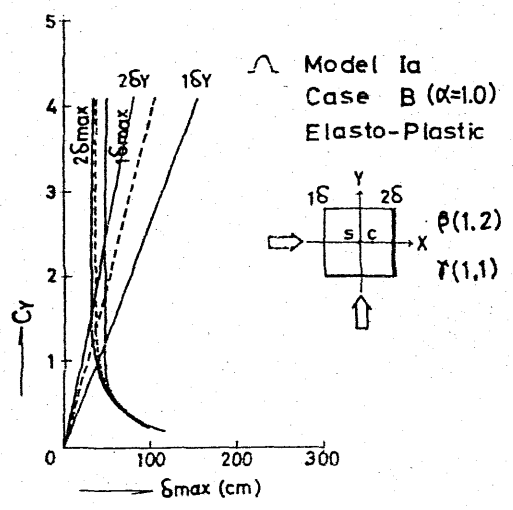

Fig.6 Relation between C_γ and δ_{max} (Model Ia, α=1.0)

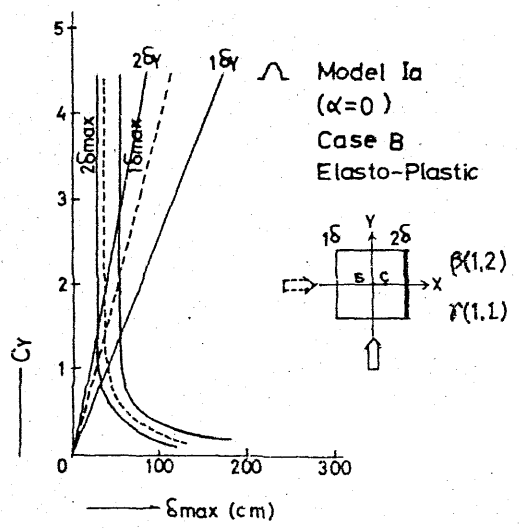

Fig.7 Relation between C_γ and δ_{max} (Model Ia α=0)

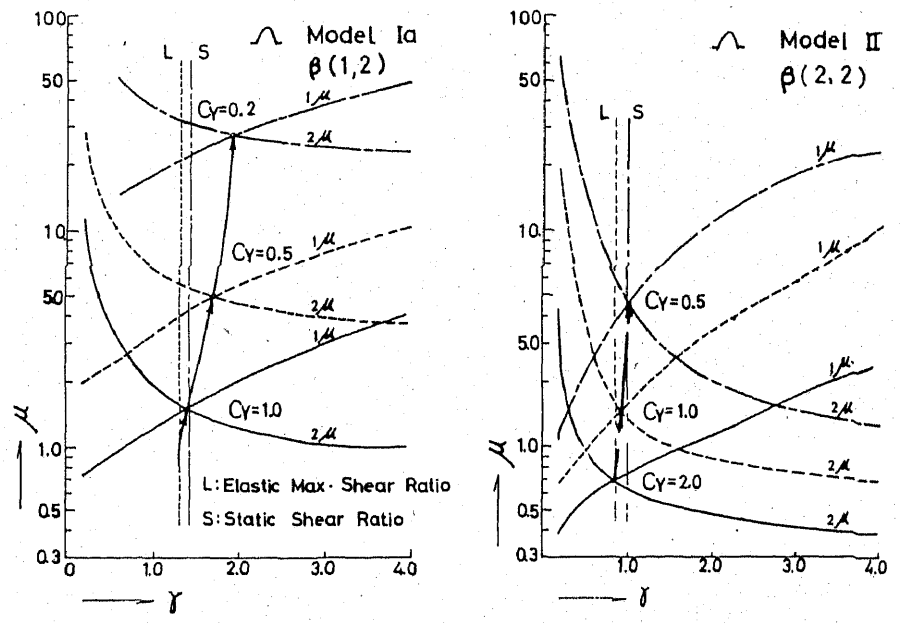

Fig. 8 Relation between Ductility Factor μ and Strength Distribution γ

Table 1. Critical Yield Level for Collapse ($k_p/k=-0.1$)

Model	Input	Case A	Case B
Symmetrical Model		0.44	
		0.32	
		0.53	
Model I β(1,2)		0.51	0.41
		0.39	0.34
		0.67	0.53
Model II β(2,2)		0.62	0.39
		0.50	0.33
		0.84	0.54

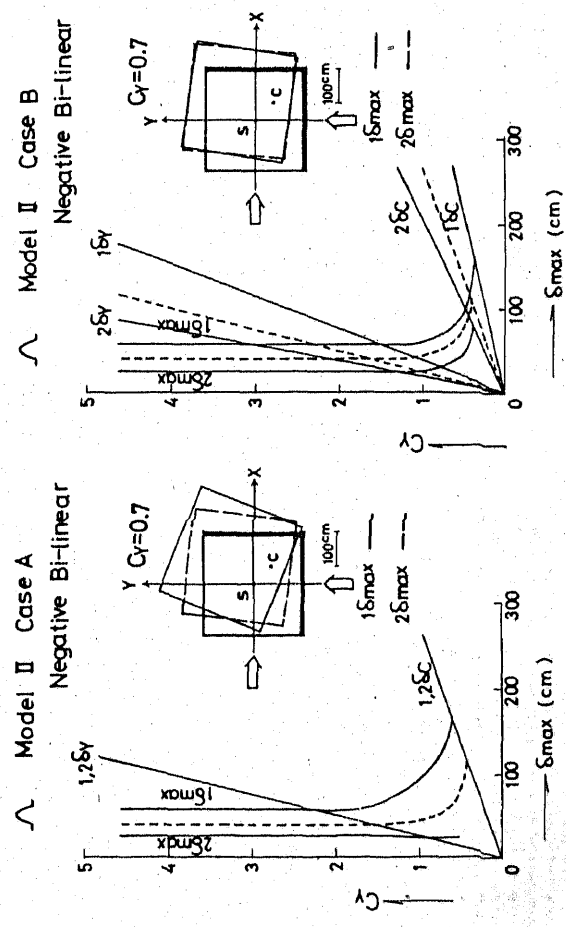

Fig. 9 Relation between Cγ and δmax (Model II, $k_p/k=-0.1$)

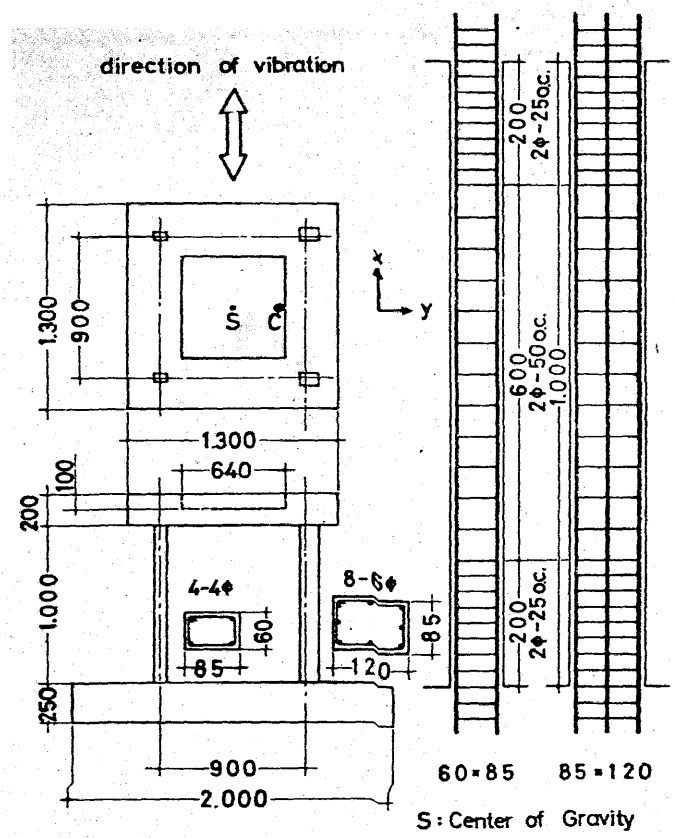

S : Center of Gravity
C : Center of Stiffness

Fig. 10. Test Specimen of AE Type

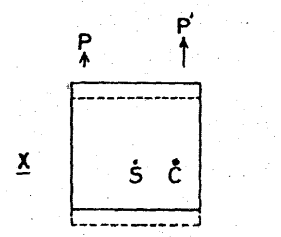

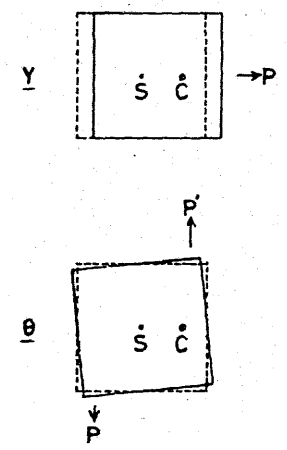

The Loading Methods in Static Test

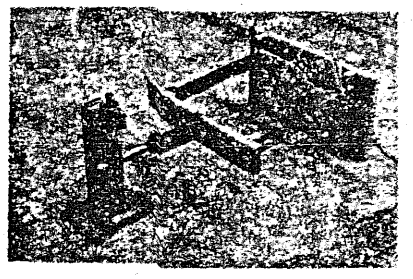

Photo 1. Deflection Transducer

Table 2. The Torsional Properties of Test Specimens

	β	γ	Cy
A-Type	1.0	1.0	0.253
AE-Type	4.0	4.03	0.734

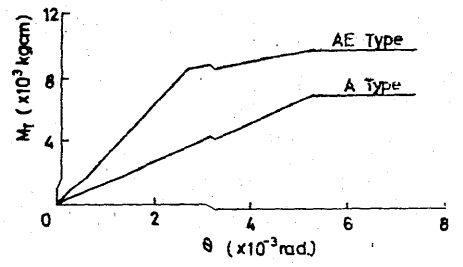

Fig. 11. Torsional Resistance Characteristics of Columns

Fig. 12.
The Torsional Moment-Rotation Angle Relation from Static Test

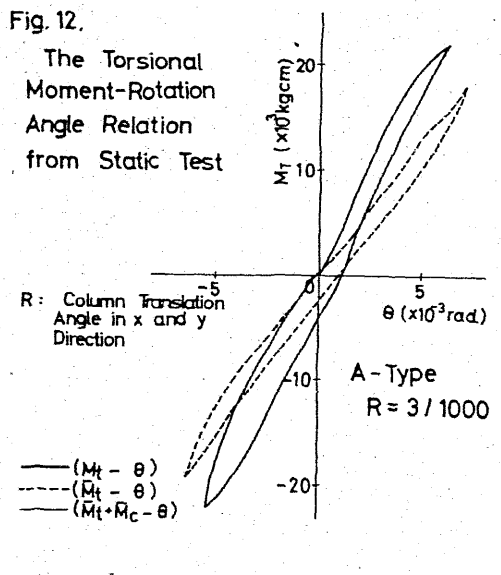

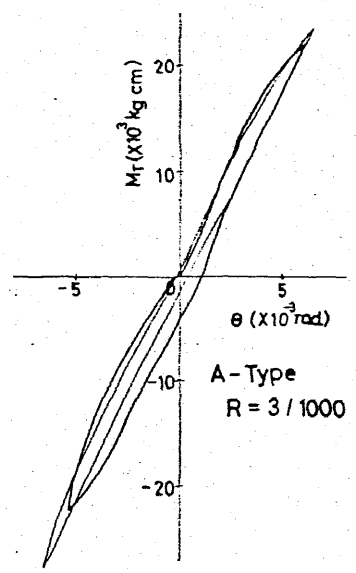

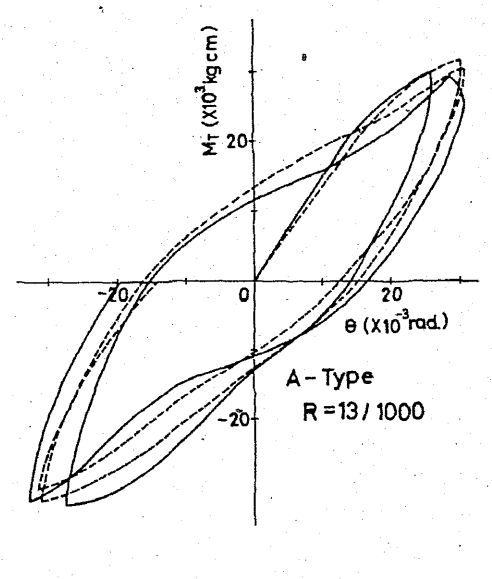

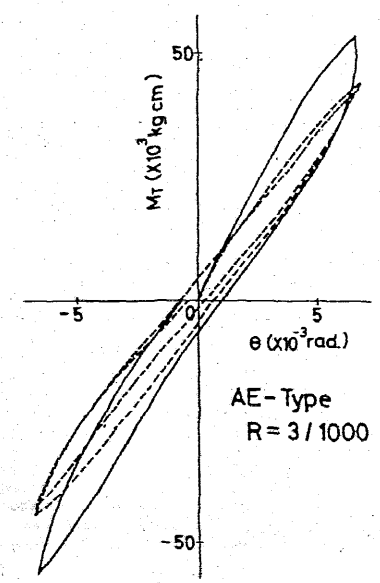

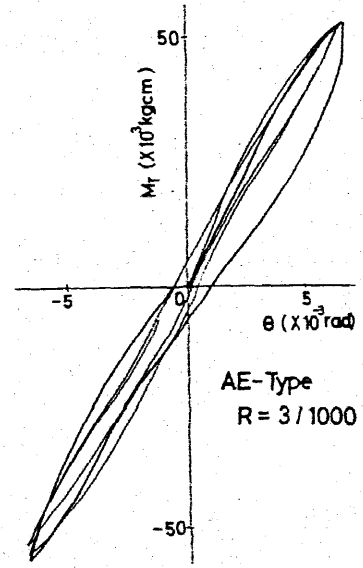

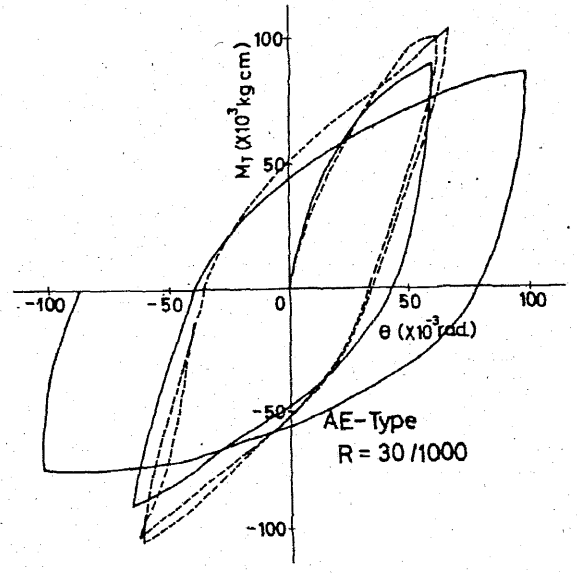

Fig. 13.
Mode Shapes
in Vibration

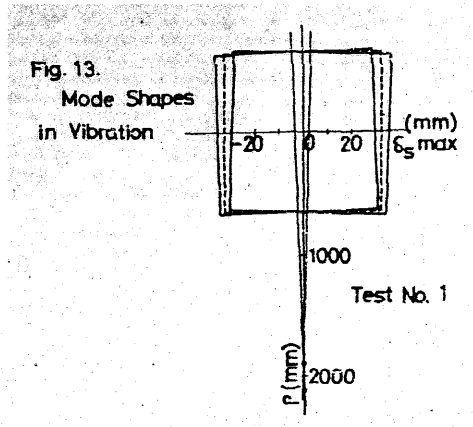

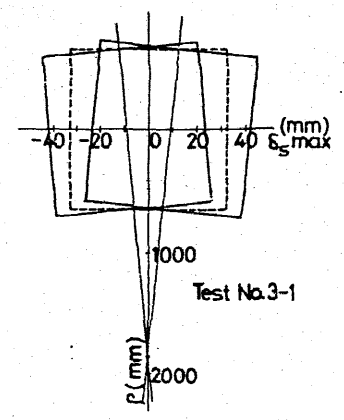

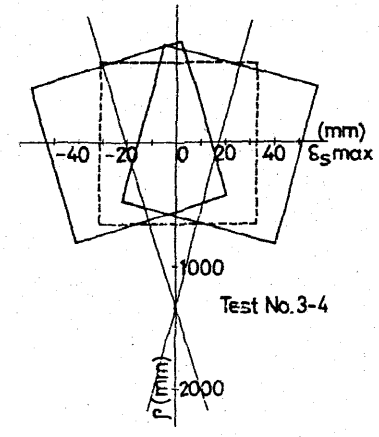

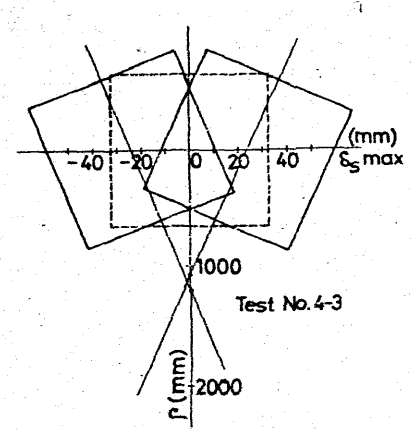

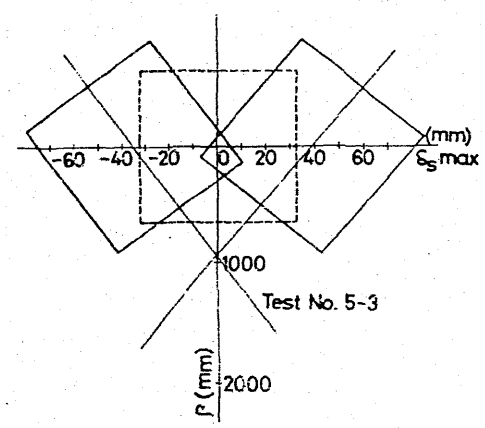

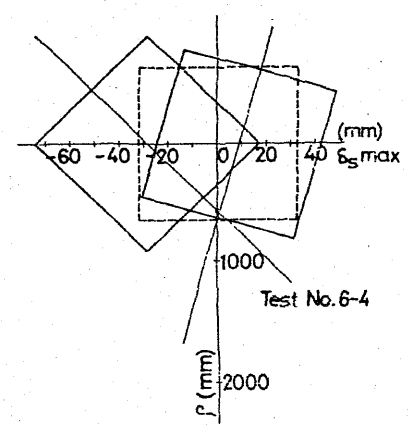

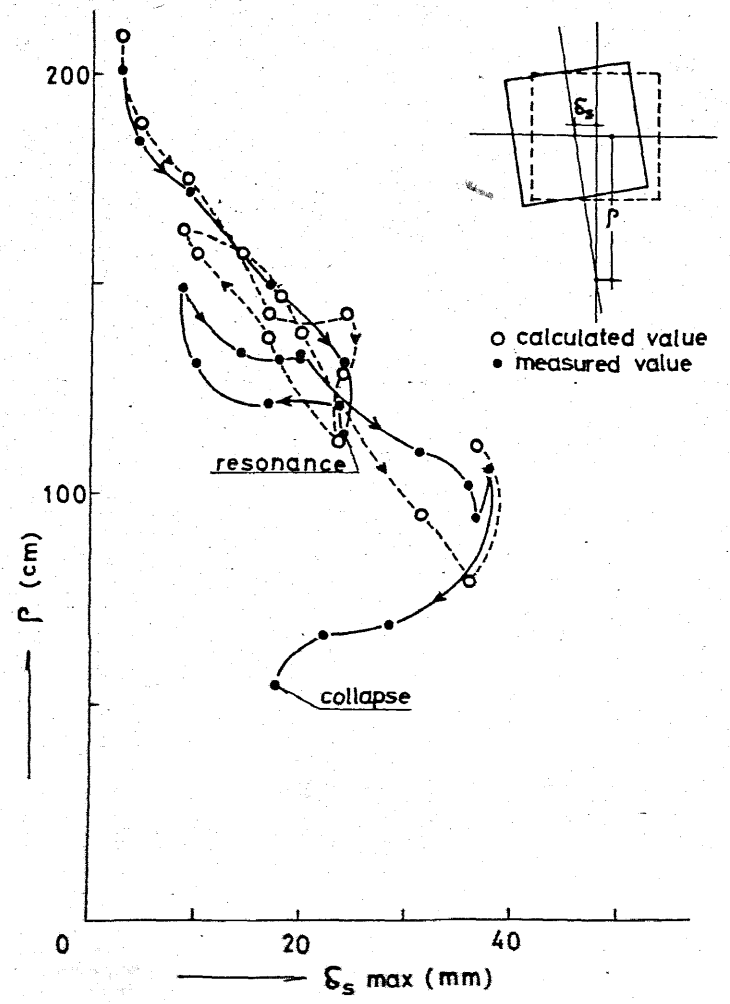

Fig.14. Relation between $\delta_s$max & P

Table 3. Results of AE-Type Specimen in Dynamic Tests

Test No.	T force (sec)	δ_s max. (mm)	θ max. (x10^{3}rad.)	P meas. (cm)	P cal (cm)	Note
1	0.62	2.8	1.4	201.1	209.0	
2	0.38	4.5	2.5	183.6	188.2	
3-1	0.32	9.2	5.7	172.2	175.0	
2	0.32	17.1	13.7	149.6	142.0	
3	0.32	24.2	27.5	131.2	142.0	
4	0.34	24.1	22.0	113.8	128.0	resonance
5	0.42	23.7	19.7	120.5	111.9	
6	0.47	16.9	14.7	120.8	137.0	
7	0.56	10.3	9.7	131.3	157.0	
8	0.66	8.8	8.8	148.4	162.5	
4-1	0.66	14.4	12.0	133.3	157.1	
2	0.57	17.9	16.0	131.2	147.0	
3	0.53	19.8	15.8	132.0	138.8	
4	0.53	19.8	16.4	132.8	138.8	
5-1	0.44	31.5	31.3	109.8	95.4	
2	0.42	36.2	40.1	101.4	79.0	
3	0.53	36.8	41.1	94.0	110.9	
6-1	0.65	37.8	38.3	105.4	—	
2	0.57	28.6	41.7	69.4	—	
3	0.55	22.2	37.8	66.8	—	
4	0.65	17.9	49.9	54.5	—	collapse

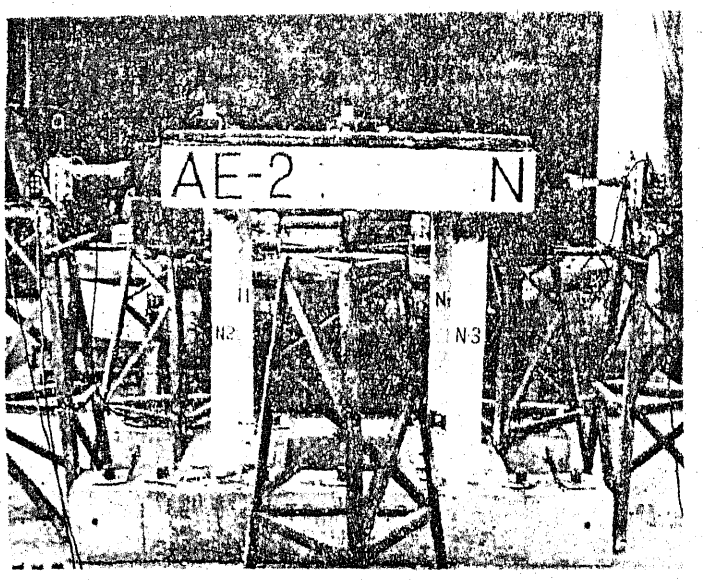

Photo. 2. Test Specimen of Dynamic Test

Photo. 3. After Dynamic Test